AutoSWIR: A SPECTRAL UNMIXING ALGORITHM USING 2000-2400 nm ENDMEMBERS AND MONTE CARLO ANALYSIS

Gregory P. Asner[1] and David B. Lobell[1]

1. Introduction

Dynamic climate and land use in arid and semi-arid systems result in complex spatial and temporal variation of vegetation properties. Large-scale monitoring is critical for assessments of ecological change in these regions (UNEP, 1992). The tight coupling of vegetation cover to important hydrological and biogeochemical processes (Schlesinger et al, 1996, Schlesinger and Pilmanus, 1998) emphasizes the paramount importance of resolving vegetation and bare soil extent for functional analyses of these environments. However, the spatial extent of vegetation and bare soils is notoriously difficult to measure in arid and semi-arid ecosystems using satellite imagery because variation occurs on the scale of a few meters or less.

Imaging spectrometry provides near-contiguous, narrow-band spectral analysis of the land surface that has proven useful for studying a wide variety of biophysical and geological processes (Green et al, 1998). One of the most common uses of imaging spectrometry is spectral mixture analysis, which capitalizes on unique spectral features of surface properties to estimate the sub-pixel cover fraction of specific land-surface types (Smith et al, 1994, Wessman et al, 1997). A central assumption is that land-cover endmembers sum linearly, or that departures from this assumption can be accommodated via residual cover fraction estimates or through the use of spectral endmember bundles. This approach has proven useful for studying various geological properties of arid and semi-arid regions due to the distinct spectral signatures of constituent rock and soil minerals (Goetz et al, 1985). An important aspect of this approach is that the spectral properties of minerals are very consistent, allowing mixture modeling approaches to readily employ library endmembers (Clark, 1999).

In comparison to minerals, the spectral properties of live and senescent plant canopies are much less consistent. Variation in the condition, amount and architectural orientation of plant tissues create canopy-level spectral variation that cannot be easily predetermined in a spectral library. It is this variation that motivates much of the biophysical remote sensing community whose goals include monitoring the dynamics of vegetation phenology, greenness, leaf area, and energy absorption (Field et al, 1995, Myneni et al, 1997, Running et al, 1994). While the condition, amount, and architectural placement of the tissues can all contribute to variability in canopy reflectance, in reality, a subset of variables tend to dominate the variation within any given ecosystem or landscape (Asner 1998). In arid and semi-arid ecosystems, the amount of green and senescent foliage accounts for most of the spatial and temporal variation in canopy-level reflectance and energy absorption (van Leeuwen et al, 1997, Asner et al, 1998b). In addition, surface moisture and roughness strongly affect the soil reflectance (Jacquemoud et al, 1995, Pinty et al, 1998). Thus, vegetation and soil spectral endmembers collected in the field are difficult to apply in spectral mixture analyses at the spatial scales needed for regional monitoring efforts.

Several spectral unmixing approaches have been developed to address variation in vegetation and soil endmember spectra (Bateson et al, 1998, Roberts et al, 1998, Smith et al, 1994). The most flexible approaches derive ranges of spectral endmembers from field data or image pixels, and then incorporate this variability into sub-pixel cover estimates (Bateson et al, *in press*). Efforts to incorporate endmember variability (e.g., via fuzzy endmember sets or bundles) are physically consistent with the natural variability that occurs among vegetation and soil spectra, but broad variation in endmembers often leads to wide ranges of plausible cover fraction results. Therefore, it is desirable to establish features of the spectrum which, for the most common land-cover types, display the least spectral variability while remaining distinct from one another.

Previous work involving arid and semi-arid vegetation in North and South America indicated high spectral variability of live and senescent canopies (Asner, 1998, Asner et al, 2000). Most of this variation was attributed to the spatial and temporal heterogeneity of leaf and litter area index (LAI, LitterAI). Similarly, it was observed that soil reflectance varied within and between sites due primarily to moisture content. However, among the sites visited in

[1] Department of Geological Sciences and Environmental Studies Program, University of Colorado, Boulder, CO

those studies, there were consistent spectral derivatives for green vegetation, litter and bare soils in the shortwave-infrared region between 2100 and 2400 nm (the "SWIR2" region). Although the overall reflectance of each cover type varied sharply within and across sites and the spectral derivatives varied throughout most of the visible and near-infrared, the SWIR2 spectral derivatives varied little and were distinct between land-cover types (Figure 1).

The consistency of the SWIR2 derivative spectra of green vegetation canopies results from foliar water acting as a very strong absorber of SWIR2 radiation (Wooley, 1971, Ustin et al, 1999). At LAI values of 1.0, the SWIR2 region nearly saturates at the reflectance values typical of green vegetation, and the SWIR2 derivative spectra are consistent at LAI of 1.0 and greater (Asner, 1998). The distinct features in SWIR2 litter reflectance result from stretching, bending, and overtones of C-H and O-H bonds associated with organic carbon compounds interacting with shortwave radiation (Curran, 1989). Soil spectra collected by Asner (1998) had a distinctive absorption feature centered near 2200 nm, which results from combinations and overtones of hydroxyl absorption in the clay lattice structure of soils that dominate many arid and semi-arid environments (Ben-Dor et al, 1999). Although the SWIR2 soil spectra varied with mineralogy and clay content (cf., Drake et al, 1999), this variation was limited to a much smaller range of values in the spectral derivatives. While the overall reflectance of both litter canopies and bare soils varied sharply from place to place, their SWIR2 derivative spectra were consistent and distinct.

Based on these earlier observations, we sought to capitalize on the apparent consistency of the SWIR2 derivatives by developing a spectral unmixing algorithm to estimate vegetation and bare soil extent in arid and semi-arid regions. Our approach was based on a three-component effort: (1) an expanded spectral survey of green vegetation, standing and surface litter, and bare soils at 17 representative sites in North and South America, (2) establishment of a reliable set of SWIR2 spectral signatures for each dominant land-cover types found in arid and semi-arid regions, and (3) development of a fast, automated spectral unmixing approach that includes statistical estimation of uncertainty in the derived sub-pixel cover fractions.

2. Methods
2.1 Field Spectroscopy

To develop a broadly applicable spectral unmixing approach for arid and semi-arid ecosystems, our strategy was to first quantify the biogeophysical variability of the dominant endmembers at as many field sites and under as many conditions as we thought necessary to ultimately acquire statistical confidence in the sub-pixel cover fractions. Recognizing the multitude of highly variable green and senescent plant canopies and bare soil in these regions, we felt that a thorough survey of their spectral properties would yield the most generalizable endmember data set needed to establish the most predictable spectral region for mixture modeling. The field spectral survey included vegetation types from grasslands, shrublands, woodlands, and savannas in desert, semi-desert, temperate, sub-tropical and tropical climates (Table 1). The data set included green and litter canopies of more than 450 herbaceous and woody plant species representing a wide array of growthforms, physiologies, canopy architectures, intra-canopy shading, tissue chemistries, and tissue optical properties (Asner, 1998, Asner et al, 2000, and *unpub. data*). Leaf area index (LAI) ranged from 0.2-7.9 among green canopies, while litter area index (litterAI) varied from 0.3-6.6 for senescent herbaceous canopies.

The data were collected using a full-range (350-2500 nm) spectrometer with an 18° sensor fore-optic (Analytical Spectral Devices, Inc.). This instrument collects data in 1.4 nm intervals from 350-1100 nm and 2.2 nm intervals in the remaining shortwave-infrared (1100-2500nm). All measurements were collected within one hour of local solar noon on clear sky days. The sensor was held 1.5 m above the top of each canopy or soil surface in the nadir position. A ladder was used to obtain spectra of large shrubs and trees at some of the sites. Radiance measurements were converted to reflectance using a Spectralon (Labsphere, Inc.) calibration panel, which was measured immediately before each canopy or soil measurement.

The 98,423 spectrum database was analyzed to find which wavelength region was most consistent for use in a generalized spectral unmixing model. Endmember bundles were then constructed to represent the variability in the selected wavelength region. Final preparation of the endmember sets included high-frequency filtering and linear transformation to emphasize spectral shape. Two possibilities were considered for characterizing spectral shapes: derivative spectra and "tied" spectra, the latter defined as subtracting the value at one wavelength (the tie point) from all other wavelengths. As will be demonstrated, the tied spectra can be advantageous because they are less sensitive to very narrow-band noise which can arise in derivative data.

2.2 Spectral Mixture Analysis

Most spectral mixture models represent the reflectance of an image pixel as the linear combination of endmember spectra:

$$\rho_{pixel} = \Sigma\ [\rho_e \bullet C_e] + \varepsilon = [\rho_{veg} \bullet C_{veg} + \rho_{soil} \bullet C_{soil} + \rho_{litter} \bullet C_{litter}] + \varepsilon \qquad (1)$$

where ρ and C are the reflectance and cover fraction of each endmember, respectively, and ε is an error term. An additional endmember is often included in these algorithms to account for the contribution of intra- and inter-canopy shadow. However, this fraction is difficult to isolate in the field or in image pixels, thus it is often used as a residual endmember. Our field experience indicated that shadow can be taken into account if the spectral database includes canopies and small areas with mixed sunlit and shaded surfaces. We also recognized that shade causes the overall reflectance of the underlying material to decrease but does not sharply alter the shape (derivatives) of the SWIR spectra. By assuming that the effects of shade on the reflectance of vegetation and soil surfaces are independent of their scale, field spectra that include a sufficiently heterogeneous mix of sunlit and shaded surfaces can account for the presence of shade at the pixel level. Both radiative transfer (for intra-canopy shade) and geometric-optical (for inter-canopy shade) theories and experiments have shown this to be a reasonable assumption (Caulfield et al, 1992, Myneni et al, 1989, Ross, 1981).

In an effort to incorporate both spectral endmember variability and uncertainty in the unmixing approach, we devised a probabilistic method using endmember sets that embodied the range of variation present in the field. A Monte Carlo unmixing (MCU) strategy was developed to derive sub-pixel cover fractions with statistical confidence intervals. The MCU approach involves generating a large number of endmember (green vegetation, litter, soil) combinations for each pixel (n=50-200 or more) by randomly selecting spectra from the database of field spectra. The performance was evaluated using raw reflectance, derivative, and tied endmember spectra. Based on a series of preliminary tests of the model, the cover fractions resulting from the MCU procedure invariably had a normal distribution for each pixel. We therefore used the mean values to estimate the fractional cover of each endmember, and the standard deviation to form a confidence interval for the true fraction. As a result, this approach allowed for a quantitative measure of how well the cover estimates were constrained using the reflectance, derivative, and tied spectral endmembers from an entirely general endmember database and in any wavelength interval.

2.3 Evaluation Using AVIRIS Imagery

The MCU approach was evaluated using Airborne Visible and Infrared Imaging Spectrometer (AVIRIS) data collected over an arid grassland-shrubland region in New Mexico. The Jornada Long-term Ecological Research (LTER) site is located near La Cruces, NM, and contains spatially complex gradients of grassland, mixed grass-shrubland, and shrubland ecosystems (see www.lternet.edu). The AVIRIS data were collected in May 1997 when most of the grasslands canopies were senescent while the shrub canopies were more green. Bare soil is ubiquitous throughout both sites, but varied in spatial extent from 1-50% in some grassland areas to 40-95% in various shrubland sites (Schlesinger et al, 1996, White et al, 2000, Asner et al, 2000). Other characteristics of the Jornada LTER site are provided in Table 1.

The AVIRIS instrument collected upwelling radiance data in 224 optical channels (~10 nm bandwidth at FWHM) covering the 380-2500 nm region. The AVIRIS was carried onboard the NASA ER-2 aircraft which flew at 20 km altitude during image acquisition, creating approximately 20m pixels. Radiance data were converted to apparent surface reflectance using the ATREM atmospheric code (Gao et al, 1993) which employs the 6S scattering code for atmospheric gases and aerosols (Vermote et al, 1996). The atmospherically-corrected AVIRIS data were compared to field spectrometer data collected at a large dry riverbed area near Sevilleta and a bare soil parking lot at Jornada. The AVIRIS and field spectrometer data were found to be statistically similar, indicating good accounting of atmospheric constituents such as aerosol and water vapor in the AVIRIS correction.

During the time of AVIRIS overflight, field spectrometric data were collected for each major land-cover type found at Jornada (Table 1). In addition, canopy and landscape structural properties were assessed using a variety of instruments and techniques. Details of the measurements and methods were provided by White et al. (2000) and Asner et al. (2000), but they included: (1) leaf area index (LAI) using both direct and indirect measurement methods, (2) vegetation cover fraction using transect surveys, quadrat analysis, digital camera, air photos, and airborne laser

altimetry techniques, (3) plant tissue optical properties using a spectrometer and integrating sphere, (4) canopy architectural properties, (5) plant height and width, and (6) species composition surveys. A subset of these measurements were used to evaluate the sensitivity of the MCU procedure to both canopy and landscape characteristics.

3. Results and Discussion
3.1 Monte Carlo Unmixing Approach

The spectral properties of green canopies, standing and surface litter, and bare soils measured at the sites listed in Table 1 were statistically similar to the subset of spectra collected by Asner (1998). Moreover, for each surface type, the spectral variability at any given site was usually equal to that of the entire data set (t-tests by wavelength, $p < 0.05$). Green canopy reflectance varied the most in the near-IR between 700-1300 nm, and the least in the SWIR2 region (Figure 2). Both litter canopy and bare soil reflectance were most variable in the SWIR (1300-2500nm); however, upon converting the data to spectral derivatives (approximated as finite differences), the most consistent spectral region was the SWIR. Green canopy spectral derivatives were also very consistent in this wavelength region. The consistency of the SWIR derivatives for each cover type indicated the strong potential for using this spectral region in a mixture decomposition of arid and semi-arid environments.

Of equal importance to the consistency of endmembers in a spectral unmixing method is the separability of those endmembers. The distinctness of each endmember largely determines the success or failure of the spectral unmixing approach. Of the possible spectral regions, the SWIR2 remained the best option for unmixing using derivative spectra. Green canopy, litter, and bare soil covers were distinct in the SWIR2 due to the features described in Figure 1. In other spectral regions, two of the dominant cover types often showed distinct and readily separable features, but only in the SWIR2 were all three endmembers consistently distinct (Figure 2). For example, the visible-NIR region provided good separation of green canopies from litter or bare soils, but differences between litter and bare soil were exceedingly difficult to detect in this part of the spectrum (also found by van Leeuwen and Huete, 1996, Asner, 1998, Asner et al, 2000). Overall, the SWIR2 spectral region provided the most consistent and distinct endmembers (as derivatives).

Based on these results, we tested the MCU procedure for estimating the fractional abundance of these cover types in simulated SWIR2 data. The mean green canopy, litter and soil spectra collected in the field were convolved to AVIRIS spectral channels and then used in a sensitivity analysis. We first investigated the effects of varying noise levels on the MCU-derived fractions using both derivative and tied spectra. Normally distributed noise with a mean of zero and a standard deviation ranging from 0-15% of the signal was added to each of four modeled spectra (each of which was a different combination of the three mean endmember spectra; Table 2). The noise represented errors that could arise from sources such as insufficient detector signal-to-noise, inaccurate atmospheric removal, and the presence of unaccounted cover types. The MCU procedure was then performed on each simulated spectrum using 100 endmember-database runs in the 2078-2278 nm wavelength interval.

In the baseline case (0% noise), both the tied and derivative methods yielded accurate fractions for each of the four modeled spectra (Table 2). However, the tied spectra were much less susceptible to noise in comparison to the derivative spectra. For example, in the case where the modeled spectra contained 80% litter, the litter fraction calculated using derivative spectra was 63% (at 15% noise level), while the fraction from the tied spectra was 78%. The results using the tied spectra were more reliable because they emphasize the broad shape of the spectra, while the derivative spectra concentrate on local differences and are thus more vulnerable to high frequency noise. Overall, the method displayed outstanding performance even at 15% noise level, which we considered to be very high and unlikely. Therefore, the tied SWIR2 spectra were adopted for use in all subsequent unmixing applications (Figure 3).

The Monte Carlo unmixing (MCU) approach was used to propagate uncertainty in endmember spectra to the final sub-pixel cover fraction results. Monte Carlo methods are popular due to their simplicity and interpretability, but they can be cumbersome if too many iterations are required to develop confident statistics. Thus, an important factor to consider was the minimum number of inversions, or runs, in the MCU needed to converge to a given mean and standard deviation. Figure 4 shows the calculated means and standard deviations from MCU performed with a varying number of runs on a spectrum modeled from equal fractions of each field endmember. The results showed that additional runs beyond 30 have little effect on the derived fractions. A conservative value of 50 runs was therefore chosen for the remainder of the study.

3.2 AVIRIS Imagery

The MCU technique was used with the tied SWIR2 spectra to estimate the fractional cover of green canopies, litter and soil in the Jornada AVIRIS scene. The relatively small standard deviations (~5%) of the cover fraction values indicated that the SWIR2 region provided the spectral endmember consistency and distinctiveness needed to estimate the sub-pixel cover fractions with statistical confidence. Had the endmembers been less consistent or distinct from one another, the Monte Carlo technique would have produced much larger standard deviation images. We tested a variety of other spectral regions, such as the visible and near-infrared, but none resulted in the narrowness and accuracy (compared to field data) of resultant endmembers as was found when using the SWIR2 region.

The resultant Jornada regional cover fractions were consistent with available GIS and vegetation maps derived from field surveys and air photos (Figures 5). For example, the Jornada results agreed with a vegetation map recently completed by LTER site personnel (Figure 5; map courtesy of B. Nolen). Green canopy cover fractions corresponded spatially with woody species such as *Prosopis glandulosa* (mesquite), which were green during the AVIRIS overflight in May 1997. Litter cover fractions were consistent with grassland areas dominated by *Boutelua eriopoda* (black grama), which was highly senescent at that time. These results also emphasized the strategic utility of acquiring imaging spectrometer data of these ecosystems in the late spring season when functionally unique vegetation types (woody and herbaceous communities) are in different phenological stages and are thus spectrally separable.

Comparison of the MCU and field-derived bare soil and vegetation fractions showed a high degree of accuracy at the site level (Figure 6). In this study, green plus senescent vegetation cover was not well correlated with the plant area index (= LAI + LitterAI) of the individual canopies (Figure 7). These results indicated that the SWIR2 region and MCU approach were primarily sensitive to the horizontal extent of vegetation types, and not to the vertical density (LAI) of the individual canopies present within pixels. Isolation of the vegetation and bare soil cover fractions within images pixels is needed for hydrological and biogeochemical analyses in arid and semi-arid regions (Asner et al, 1998a,b, Schlesinger et al, 1998). It also provides a means to monitor changes in vegetation cover associated with land-use and climate impacts such as desertification (UNEP, 1992).

We contend that the SWIR2 Monte Carlo unmixing method is robust for two reasons. First, the method provides a means to directly incorporate endmember variability into the spectral unmixing effort. Analogous methods have been used to account for endmember variability (e.g., Bateson et al, *in press*), so this development is not fully unique. However, in combination with the establishment of SWIR2 tied spectra whose selection was based on the stability of the spectral endmembers in a biogeophysically diverse field survey, our approach is both physically robust and computationally efficient, lending itself to complete automation. Our method provided verifiably accurate results without ground calibration or excessive image preparation. While we think that the approach is especially robust in arid and semi-arid vegetation and soil types, we also have strong evidence suggesting its utility in other scenarios such as forested ecosystems (Lobell et al, *in review*).

4. Acknowledgements

5. References

Asner, G.P. (1998), Biophysical and biochemical sources of variability in canopy reflectance, *Remote Sens. Environ.* 64:234-253.

Asner, G.P., Braswell, B.H., Schimel, D.S., et al. (1998a), Ecological research needs from multi-angle remote sensing data. *Rem. Sens. Environ.* 63:155-165.

Asner, G.P., Wessman, C.A., Bateson, C.A., et al. (2000), Impact of tissue, canopy and landscape factors on reflectance variability of arid ecosystems. *Rem. Sens. Environ*. In press.

Asner, G.P., Wessman, C.A., and Schimel, D.S. (1998b), Heterogeneity of savanna canopy structure and function from imaging spectrometry and inverse modeling, *Ecol. Applic*. 8:1022-1036.

Bateson, C.A., Asner, G.P. and Wessman, C.A. (1999), Endmember bundles: a new approach to incorporating endmember variability in spectral mixture analysis. *IEEE Trans. Geosci. Rem. Sens*. In press.

Bateson, C.A. and Curtiss, B. (1996), A method for manual endmember selection and spectral unmixing, *Rem. Sens. Environ.* 55:229-243.

Ben-Dor, E., Irons, J.R., and Epema, G.F. (1999), Soil reflectance. In *Remote Sensing for the Earth Sciences* (A.N. Rencz, Ed.), John Wiley and Sons, New York, pp. 111-188..

Carlson, T.N., and Ripley, D.A. (1997), On the relation between NDVI, fractional vegetation cover, and leaf area index. *Rem. Sens. Environ*. 62:241-255.

Caulfield, F., Britz, S.J., and Bunce, H.A. (1992), Shade spectral quality and the photosynthetic capacity of soybean leaves. *Photosynthetica* 26:555-568.

Clark, R.N. (1999), Spectroscopy of rocks and minerals, and principles of spectroscopy. In *Remote Sensing for the Earth Sciences* (A.N. Rencz, Ed.), John Wiley and Sons, New York, pp. 3-57.

Curran, P.J. (1989), Remote sensing of foliar chemistry. *Rem. Sens. Environ.* 30:271-278.

Drake, N.A., Mackin, S., and Settle, J.J. (1999), Mapping vegetation, soils and geology in semiarid shrublands using spectral matching and mixture modeling of SWIR AVIRIS imagery. *Rem. Sens. Environ.* 68:12-25.

Field, C.B., Randerson, J.T., and Malmstrom, C.T. (1995), Global net primary production: combining ecology and remote sensing, *Remote Sens. Environ.* 51:74-88.

Gao, B.-C., Heidebrecht, K.B., and Goetz, A.F.H. (1993), Derivation of scaled surface reflectance from AVIRIS data. *Rem. Sens. Environ.* 44:165-178.

Goetz, A.F.H., Vane, G., Solomon, J.E., and Rock, B.N. (1985), Imaging spectrometry for Earth remote sensing. *Science* 228:1147-1153.

Green, R.O., Eastwood, M.L., and Williams, O. (1998), Imaging spectroscopy and the Airborne Visible/Infrared Imaging Spectrometer (AVIRIS). *Rem. Sens. Environ.* 65:227-240.

Hall, F.G., Huemmrich, K.F., and Goward, S.N. (1990), Use of narrow-band spectra to estimate the fraction of absorbed photosynthetically active radiation. *Rem. Sens. Environ*. 32:47-60.

Jacquemoud, S., Baret, F. and Hanocq, J.F. (1992), Modeling spectral and bidirectional soil reflectance, *Rem. Sens. Envir.* 41:123-132.

Lobell, D.B., Asner, G.P., Law, B.E. and Treuhaft, R.N. Sub-pixel cover estimation of coniferous forests in Oregon using SWIR imaging spectrometry. *J. Geophys. Res.,* in review.

Myneni, R.B., Los, S.O., and Tucker, C.J. (1996), Satellite-based identification of linked vegetation index and sea surface temperature anomaly areas from 1982-1990 for Africa, Australia and South America. *Geophys. Res. Lett.* 23:729-732.

Myneni, R.B., Nemani, R.R., and Running, S.W. (1997), Estimation of global leaf area index and absorbed PAR using radiative transfer models, *IEEE Trans. Geosci. Rem. Sens*. 35:1380-1396.

Myneni, R.B., Ross, J., and Asrar, G. (1989), A review on the theory of photon transport in leaf canopies. *Agric. For. Meteor.* 45:1-153.

NMAES. (1970), Influence of grazing intensity on improvement of deteriorated black grama range. Bulletin 553. New Mexico Agricultural Experiment Station, Las Cruces, New Mexico.

Pinty, B., Verstraete, M.M., and Gobron, N. (1998), The effect of soil anisotropy on the radiance field emerging from vegetation canopies. *Geophys. Res. Lett.* 25:797-800.

Ross, J.K. (1981), *The Radiation Regime and Architecture of Plant Stands*. Kluwer Academic, Boston, MA.

Running, S.W., Justice, C.O., Salomonson, V., et al. (1994), Terrestrial remote sensing science and algorithms planned for EOS/MODIS. *Int'l J. Rem. Sens.* 15:3587-3620.

Schlesinger, W.H., and Pilmanis, A.M. (1998), Plant-soil interactions in deserts. *Biogeochemistry* 42:169-87.

Schlesinger, W.H., Raikes, J.A., and Cross, A.F. (1996), On the spatial pattern of soil nutrients in desert ecosystems. *Ecology* 77:364-376.

Schlesinger, W.H., Reynolds, J.F., Cunningham, G.L., et al. (1990), Biological feedbacks in global desertification. *Science* 247:1043-1048.

Smith, M.O., Adams, J.B., and Sabol, D.E. (1994), Spectral mixture analysis-new strategies for the analysis of multispectral data. In *Imaging Spectrometry-A Tool for Environmental Observations* (J. Hill and J. Megier, Eds.), Kluwer Academic, Dordrecht, The Netherlands, pp. 125-144.

Stoner, E.R., and Baumgardner, M.F. (1981), Characteristic variations in reflectance of surface soils. *Soil Sci. Soc. Am. J.* 45:1161-1165.

Tucker, C.J., Dregne, H.E., and Newcomb, W.W. (1991), Expansion and contraction of the Sahara Desert from 1980 to 1990. *Science* 253:299-301.

UNEP (1992), *Status of Desertification and Implementation of the United Nations Plan of Action to Combat Desertification*. United Nations Environment Programme, Nairobi, Kenya.

USDA (1934), The influence of precipitation and grazing on black grama range. Technical Bulletin 409, U. S. Department of Agriculture.

Ustin, S.L., Smith, M.O., Jacquemoud, S., et al. (1999), Geobotany: vegetation mapping for earth sciences. In *Remote Sensing for the Earth Sciences* (A.N. Rencz, Ed.), John Wiley and Sons, New York.

van Leeuwen, W.J.D. and Huete, A.R. (1996), Effects of standing litter on the biophysical interpretation of plant canopies with spectral indices, *Remote Sens. Environ.* 55:123-134.

Vermote, E.F., et al. (1996), Second simulation of the satellite signal in the solar spectrum, 6S: an overview. *IEEE Trans. Geosci. Rem. Sens*. 35:675-699.

Wessman, C.A., and Asner, G.P. (1998), Ecosystems and the problems of large-scale measurements. In *Successes, Limitations, and Frontiers in Ecosystem Ecology* (P. Groffman and M. Pace, Eds.), Springer-Verlag, Berlin, pp. 346-371.

Wessman, C.A., Bateson, C.A., and Benning, T.L. (1997), Detecting fire and grazing patterns in tallgrass prairie using spectral mixture analysis, *Ecol. Appl.* 7:493-511.

White, M.A., Asner, G.P., Nemani, R.R., et al. (2000), Monitoring fractional cover and leaf area index in arid ecosystems: digital camera, radiation transmittance, and laser altimetry results. *Rem. Sens. Environ.* In press.

Wooley, J.T. (1971), Reflectance and transmittance of light by leaves. *Plant Physiol.* 47:656-662.

Table 1. Description of field sites visited to collect canopy and bare soil endmember spectra.

Ecosystem/Vegetation Type	Site Location	Annual Precipitation[2]	Dominant Soil Type	Canopy-level LAI Range[3]
Desert Grassland	Jornada LTER[1], NM	230	Aridisols	0.1-0.8
Desert Scrub/Shrubland	Jornada LTER, NM	230	Aridisols	0.9-3.1
Arid Grassland	Sevilleta LTER, NM	255	Entisols	0.2-1.6
Desert Shrubland, Shrub-Steppe	Sevilleta LTER, NM	255	Entisols	0.8-3.9
Desert Scrub/Shrubland	Tucson, AZ	290	Aridisols	0.6-4.4
Semi-arid Shortgrass Prairie	Colorado Springs, CO	385	Alfisols/ Mollisols	0.4-1.7
Semi-arid Woodland	Colorado Springs, CO	402	Entisols	0.6-4.4
Semi-arid/Temperate Tallgrass Prairie	Boulder, CO	485	Alfisols	0.5-3.6
Semi-arid Shrubland/ Woodland	Sonora, TX	575	Alfisols/ Entisols	0.6-4.9
Xeromorphic Woodland	San Carlos, CA	605	Entisols	1.1 -5.6
Annual Grassland	San Carlos, CA	611	Entisols	0.6-3.7
Temperate Tallgrass Prairie	Vernon, TX	640	Mollisols/ Entisols	0.3-4.2
Temperate Savanna	Vernon, TX	640	Mollisols/ Entisols	0.9-5.1
Sub-tropical Savanna	Alice, TX	720	Alfisols/ Ultisols	0.7-5.4
Tropical Savanna	Brasilia, Brazil	1490	Ultisols/ Oxisols	0.4-3.2
Tropical Woodland	Brasilia, Brazil	1490	Ultisols/ Oxisols	0.7-4.8
Tropical Grassland	Brasilia, Brazil	1490	Oxisols/ Ultisols	0.6-6.9

[1] NSF Long-term Ecological Research Sites; [3] Values in mm; [2] Measured using Licor LAI-2000 Instrument

Table2. Effect of noise on calculated cover fractions using tied and derivative spectra. Four different spectral mixing scenarios were tested. Specified noise level signifies the standard deviation of normally distributed noise as a percent of the modeled spectra at each wavelength.

| Modeled Fractions	Noise Level	Litter Fraction		Leaf Fraction		Soil Fraction	
		Tied	Derivative	Tied	Derivative	Tied	Derivative
(a) litter = .333	0%	0.34	0.34	0.33	0.33	0.34	0.34
green canopy = .333	5%	0.34	0.33	0.33	0.34	0.34	0.34
soil = .333	10%	0.33	0.34	0.33	0.32	0.34	0.34
	15%	0.32	0.24	0.33	0.42	0.35	0.34
(b) litter = 0.8	0%	0.82	0.81	0.08	0.10	0.10	0.09
green canopy = 0.1	5%	0.81	0.79	0.09	0.12	0.10	0.09
soil = 0.1	10%	0.80	0.80	0.09	0.11	0.10	0.09
	15%	0.78	0.63	0.11	0.28	0.11	0.09
(c) litter = 0.1	0%	0.11	0.12	0.80	0.77	0.09	0.11
green canopy = 0.8	5%	0.11	0.11	0.80	0.78	0.10	0.11
soil = 0.1	10%	0.11	0.11	0.80	0.78	0.10	0.11
	15%	0.11	0.08	0.80	0.81	0.09	0.10
(d) litter = 0.1	0%	0.09	0.08	0.10	0.11	0.82	0.81
green canopy = 0.1	5%	0.09	0.08	0.10	0.11	0.82	0.81
soil = 0.8	10%	0.08	0.09	0.10	0.08	0.83	0.83
	15%	0.07	0.01	0.10	0.16	0.84	0.83
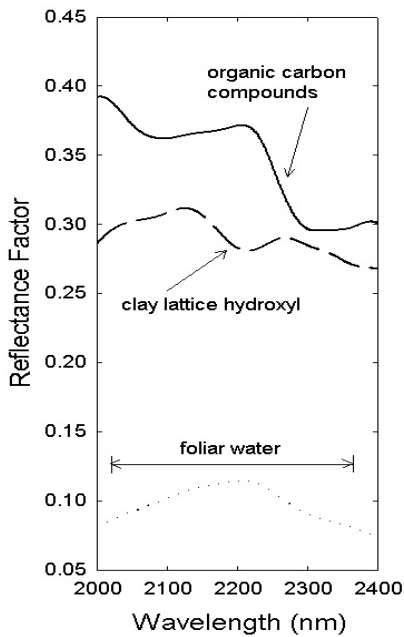
Figure 1. Typical spectra of green canopy (dotted), litter (solid), and bare soil (dashed) in SWIR2 region (2000-2400 nm). Primary causes of major spectral features are provided.
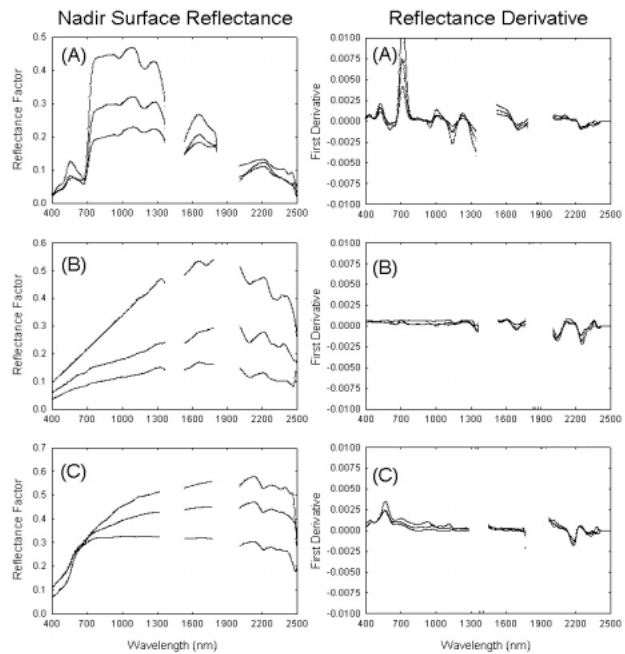

Figure 2. Sample nadir reflectance and derivative spectra (400-2500 nm) of green and senescent (litter) canopies and bare soils collected at 17 arid and semi-arid sites in North and South America. Full range of variability is shown.
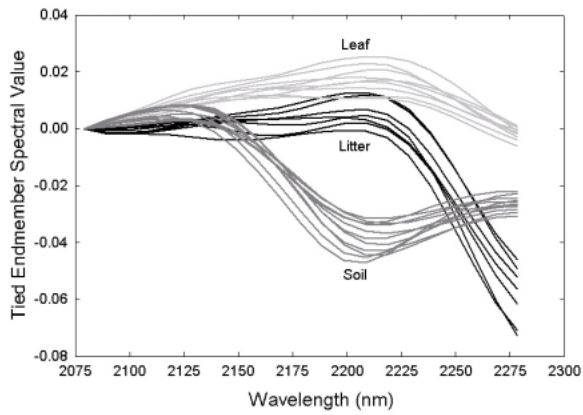
Figure 3. Examples of SWIR2 tied-endmember spectra, showing full range of variability within endmember classes.
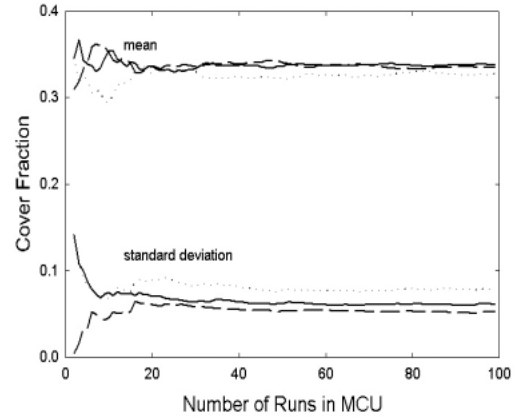
Figure 4. Mean and standard deviation of canopy (dotted), litter (solid), and bare soil (dashed) fractions versus number of runs in the Monte Carlo Unmixing (MCU) algorithm.
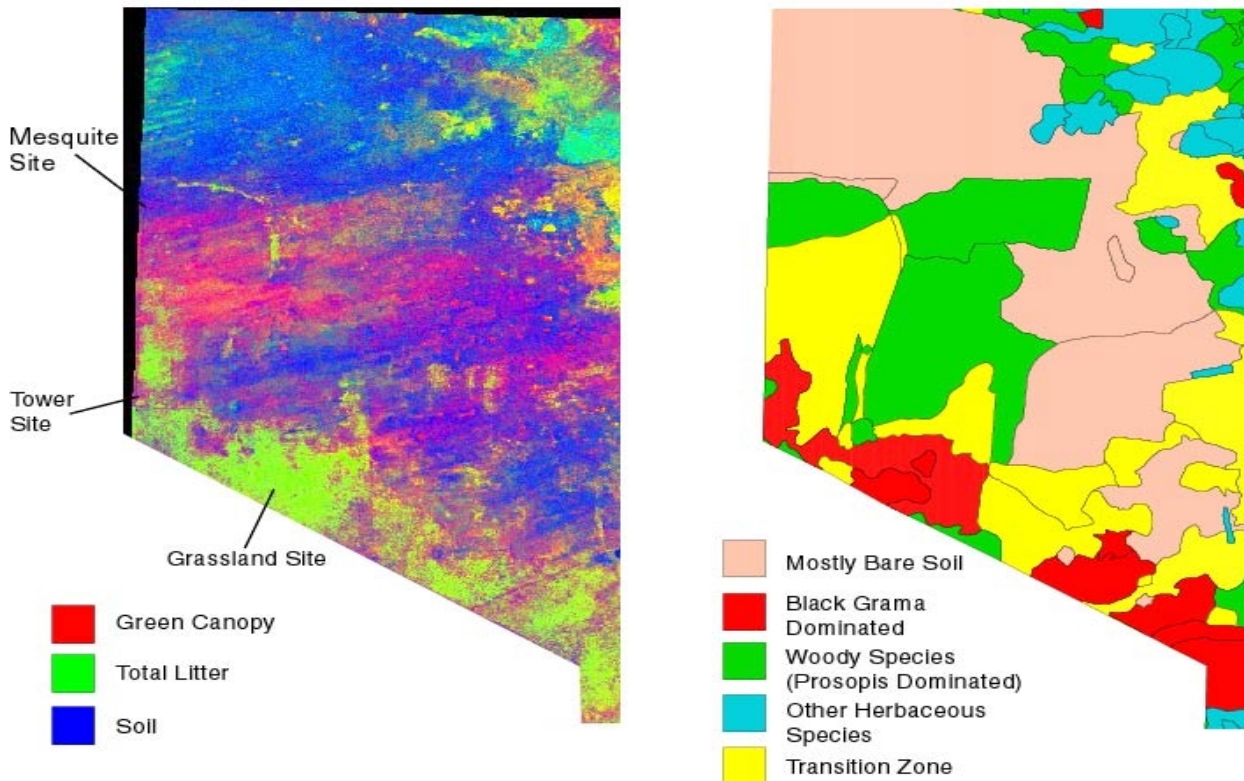

Figure 5. Composite of true green canopy, total litter, and bare soil fractions in comparison to a field-based vegetation map for Jornada LTER site, NM. Locations and names of field sites are also shown. Vegetation map courtesy of B. Nolen.
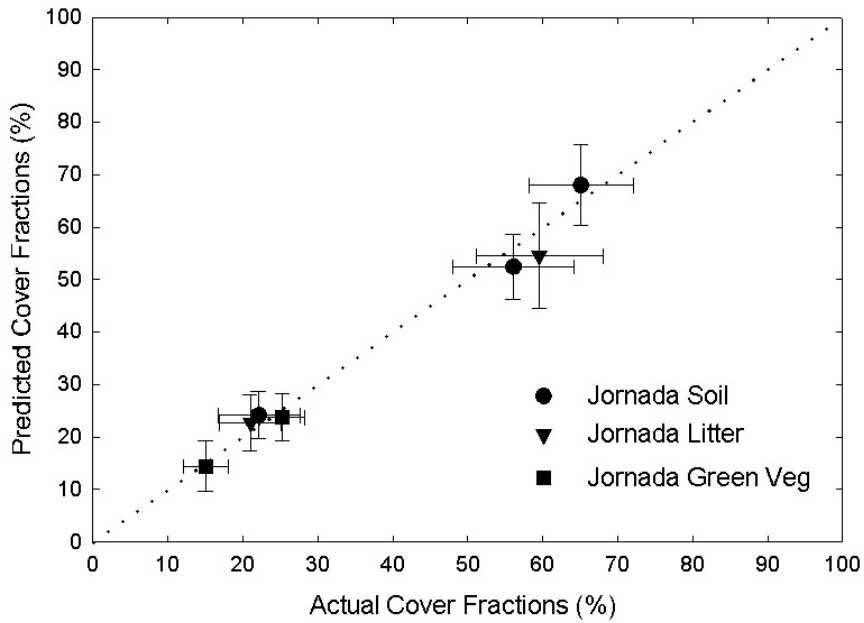
Figure 6. Comparison of actual and predicted cover fractions from field sites at Jornada LTER site, NM. Vertical error bars indicated Monte Carlo uncertainty. Horizontal error bars represent uncertainty in field measurements.
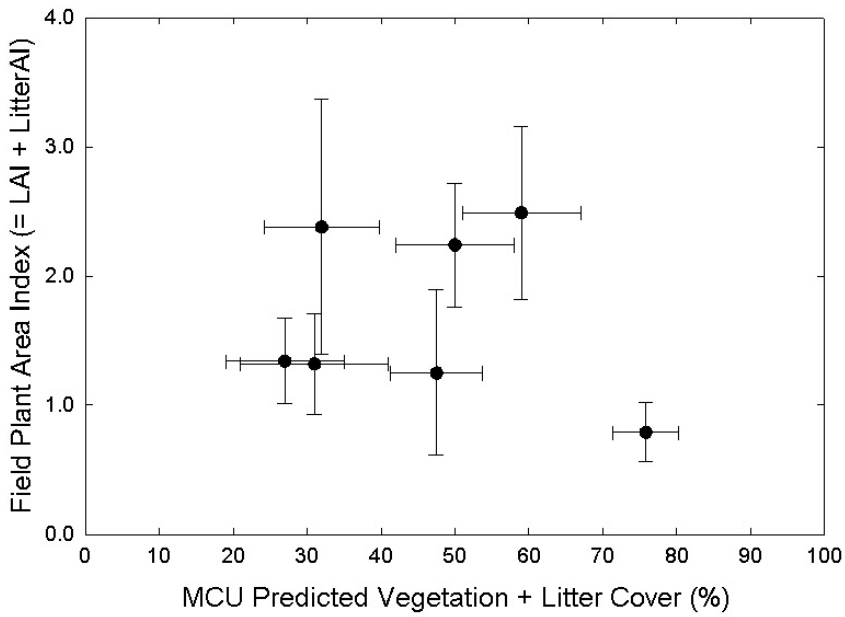

Figure 7. Comparison of predicted cover fraction and total plant area index (= leaf + litter area index) collected at Jornada LTER site, NM.